ITC 2/52
Information Technology and Control
Vol. 52 / No. 2 / 2023
pp. 562-575
DOI 10.5755/j01.itc.52.2.32690

Efficient and Accurate Vehicle Localization Based on LiDAR Place Recognition

Received 2022/11/08 | Accepted after revision 2022/12/13

HOW TO CITE: Qimin, X., Xin, Z., Longjie, L., Yameng, L., Na, L. (2023). Efficient and Accurate Vehicle Localization Based on LiDAR Place Recognition. *Information Technology and Control,* 52(2), 562-575. https://doi.org/10.5755/j01.itc.52.2.32690

Efficient and Accurate Vehicle Localization Based on LiDAR Place Recognition

Xu Qimin

Key Laboratory of Technology on Intelligent Transportation Systems, Ministry of Transport, Beijing, China.
School of Instrument Science and Engineering, Southeast University, Nanjing, China

Zhao Xin

School of Instrument Science and Engineering, Southeast University, Nanjing, China

Liao Longjie

School of Instrument Science and Engineering, Southeast University, Nanjing, China

Li Yameng, Li Na

Key Laboratory of Technology on Intelligent Transportation Systems, Ministry of Transport, Beijing, China

Corresponding author: jimmy.xqm@gmail.com

An efficient and accurate LiDAR place recognition methodology is proposed for vehicle localization. First, the Iris-LOAM is proposed to overcome the disadvantages of low accuracy of loop-closure detection and low efficiency of map construction in the existing LOAM-series methods. The method integrates the LiDAR-Iris global descriptor and Normal Distribution Transform (NDT) registration method into the loop-closure detection module of LiDAR Odometry and Mapping (LOAM), thereby improving the accuracy and efficiency of map construction. For the shortcomings of low map loading and matching efficiency, the Random Sample Consensus method is used to remove the ground point cloud information. The Voxel Grid method is used to down sample the loaded map. Finally, the NDT method is adopted for point cloud map matching to obtain the position information. Show that the Iris-LOAM has higher efficiency than the SC-LeGO-LOAM. The average time of point cloud map matching is reduced by 39.5%. The place recognition can be executed to achieve accuracy vehicle localization.

KEYWORDS: Intelligent Transportation System (ITS), LiDAR-based SLAM, Iris-LOAM, NDT matching.

1. Introduction

Accuracy vehicle position information is one of the basic key technologies for the effective operation of the ITS [1, 12]. The traditional methods of vehicle positioning are mainly based on the Global Navigation Satellite System (GNSS), including Beidou of China, Global Positioning System (GPS) of the United States, and Global Navigation Satellite System (GLONASS) of Russia [6]. However, affected by tall buildings, trees, interchanges, tunnels, etc., GNSS always cannot achieve good performance when the satellite signals are blocked [15]. The GNSS/Inertial Navigation System (INS) integrated positioning method is often utilized to provide continuous position information during GNSS outages [3, 8]. However, in complex environments, frequent signal occlusion of GNSS and severe accumulative errors of the INS make it difficult to guarantee the positioning accuracy of the traditional GNSS/INS integrated system.

Recent years, with the reduction of LiDAR cost and the rise of Simultaneous Localization and Mapping (SLAM) technology, LiDAR-based SLAM technology has earned more and more attentions. The traditional SLAM technology uses the characteristics of the external environments to calculate the relative motion and resulting in the high requirements for the external environments. When the environmental features are sparse, the extracting of feature points or calculating of relative motion may fail. The positioning accuracy will also decrease with the increase of vehicle driving distance. However, the method of place recognition is less affected by the external environments. The accurate point cloud map is established in advance, then, the position information is achieved by map matching. The place recognition method [7] is very suitable for the localization task in factory, industrial park, and other areas with pre-defined route.

For the mapping method, the LOAM [17] is one of the famous methods to use the LiDAR point cloud to solve the problem of constructing a 3D map in SLAM. However, LOAM suffers from accumulative errors because it does not have loop-closure detection part. Lightweight and Groud-Optimized LiDAR Odometry and Mapping (LeGO-LOAM) [11] is an upgrade version of LOAM. It utilizes lightweight feature extraction and adds the loop-closure detection part. Besides, Kim Giseop et al. combined the Scan Context (SC) and Lego-LOAM to propose SC-LeGO-LOAM [14]. This method retains the original features of the point cloud to improve the robustness and loop-closure detection speed of LeGO-LOAM. SC-LeGO-LOAM has the advantages of good global consistency and computational efficiency. However, the method only uses the maximum height information of the point cloud and ignore other useful information.

In this paper, an efficient and accurate vehicle localization methodology is proposed by using LiDAR place recognition. First, an improved Iris-LOAM method is proposed to construct the point cloud map with good global consistency and high accuracy. The LiDAR-Iris global descriptor is adopted to filter out several loop-closure frames and then the NDT registration method [10] is used to determine the true loop-closure frame. Thus, the efficiency of loop-closure detection can be improved. After that, in order to improve the matching speed while ensuring the matching accuracy, the point cloud map is gridded and voxelized when loading, and the Random Sample Consensus (RANSAC) algorithm is adopted to remove the ground point cloud information.

The main contribution of this paper can be summarized as the following: The efficiency of traditional LiDAR place recognition is improved from two aspects of map construction and matching. LiDAR-Iris based loop-closure detection is introduced into the construction procedure of point cloud map. Besides, the point cloud matching and positioning is optimized through efficient map loading and ground point cloud removing. Meanwhile, the accuracy of vehicle localization is maintained at a high level.

The organization of the paper is as follows. Section 2 explains the detailed implementation of Iris-LOAM based point cloud map construction. Section 3 describes the procedure of vehicle localization based on point cloud map matching. Section 4 presents the results of experimental validation while Section 5 presents the concluding remarks.

2. Iris-LOAM Based Point Cloud Map Construction

The construction of a high-precision 3D map using the point cloud collected by LiDAR is an important basis for the accurate estimation of vehicle localization. A high-precision 3D point cloud map can record the scene information in detail, which is beneficial to the subsequent map-based matching and positioning process.

In this section, a novel map construction algorithm called Iris-LOAM is proposed. This algorithm has the advantages of high efficiency and accuracy, the framework is shown in Figure 1. The algorithm uses the accurate and efficient LiDAR-Iris as the scene descriptor to filter out multiple keyframes for loop-closure. Further, the NDT alignment algorithm determines the loop closure keyframes.

2.1. Iris-based Loop Closure Detection

Incremental map using laser point clouds in large-scale environment inevitably generates accumulative errors. Loop closure detection is a core step towards robust map building by correlating global data based on whether the LIDAR has reached a historical scene. Loop closure detection can significantly reduce the accumulative errors and produce the point cloud map with global consistency [16].

During the loop closure detection, it is crucial to find effective and concise global descriptors. This paper uses iris [2] as the global descriptor to make sufficient and efficient use of the point cloud information. The generation process of iris is depicted as follows:

First, the pre-processed laser point cloud is converted into an iris image. Taking the square area of 80×80 m2 around the LiDAR as the horizontal field of view, the point clouds $X_{bc}=\{x_{b1},x_{b2},...,x_{bN}\}$ are divided into 80×360 grids according to the radial resolution of 1m and the angular resolution of 1° .Each grid is denoted by b_{ij}, where $i\in[1,80],j\in[1,360]$. For the mechanically rotating LiDAR with line number N, the horizontal field of view of 360°, and the vertical field of view range of $[-\theta_1,\theta_2]$, its maximum scanning height in the vertical direction (z-axis) is $z_h=z\tan\theta_2$, and the minimum scanning height is $z_h=-z\tan\theta_1$. Following the range of $[z_l,z_h]$, the point clouds are linearly discretized again into 8 lattices in the vertical direction of b_{ij}, where each lattice is $b_{ijk},k\in\{1,2,3,...,8\}$. The b_{ijk} is 1 when there is at least one point cloud data in b_{ijk}, and vice versa, $b_{ijk}=0$. According to the above encoding method, the pre-processed laser point cloud is projected as an iris image of size 80×360, and the pixels in row i and column j of the image is b_{ij}. This encoding method is more efficient as it does not need to calculate each point cloud in each grid.

To further enhance the feature representation in iris images, the LoG-Gabor filter is applied to extract features from point cloud iris images. The LoG-Gabor filter [9] processes the images in a similar process to the human eye vision system. The iris images are

Figure 1
The Framework of Iris-LOAM

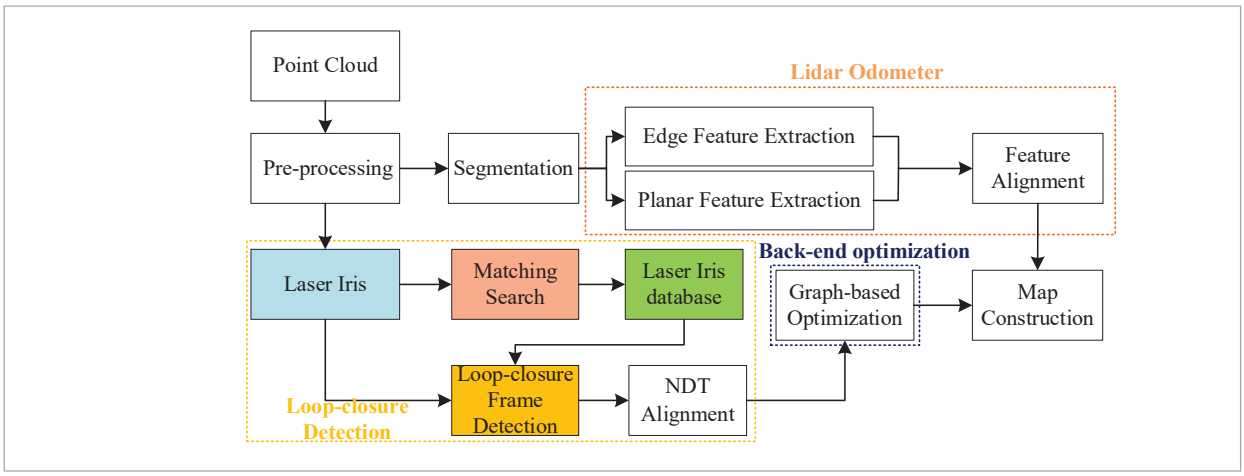

decomposed into binary feature maps with different resolutions. The features with the same location and resolution are matched, thus the accuracy of loop closure feature matching is improved.

When the vehicles pass through the same position, the spatial rotation relations of the point clouds obtained twice are projected as pixel translation relations in the image. However, the spatial translation relationship between loop closure point clouds cannot be handled using only the projected image. In other words, the projected image is not rotationally invariant. Considering that the Fourier transform can estimate the rotation, translation, and scaling in the image, the iris feature points transformed by the LoG-Gabor are processed by the Fourier transform method to get the spatial rotation and translation relations between the loop closure point clouds.

Suppose the point cloud I_1 is consistent with I_2 after the rank transformation (δ_x, δ_y), that is

$$I_1(x,y) = I_2(x-\delta_x, y-\delta_y)\cdot \tag{1}$$

The Fourier transform form of the above equation is

$$\hat{I}_1(u,v)e^{-j(u\delta_x+v\delta_y)} = \hat{I}_2(u,v)\cdot \tag{2}$$

The corresponding mutual power density spectrum is

$$\hat{C}_p = \frac{\hat{I}_1(u,v)}{\hat{I}_2(u,v)} = e^{-j(u\delta_x+v\delta_y)}, \tag{3}$$

where the inverse Fourier transform of C is

$$C_p(x,y) = F^{-1}\left(\hat{C}_p\right) = \delta(x-\delta_x, y-\delta_y), \tag{4}$$

where the mutual power density spectrum $C_p(x,y)$ at the iris image (x,y) is not zero only when $(\delta_x,\delta_y) = \underset{(x,y)}{\operatorname{argmax}}\left[C_p(x,y)\right]$. Thus, the transformation relation (δ_x,δ_y) between the iris images obtained from the projection of the point clouds at the loop closure place can be determined.

2.2. Point Cloud Map Construction

The map construction module matches the feature set $\{F_e^t, F_p^t\}$ in Y_t with its surrounding global point cloud feature map $\bar{Q}^{t-1}$, and obtains the best positional transformation between Y_t and $\bar{Q}^{t-1}$ by Levenberg-Marquardt (LM) Optimization. The process is specified as follows.

Suppose the global point cloud map at moment $t-1$ is

$$M^{t-1} = \{\{F_e^1, F_p^1\}, \{F_e^2, F_p^2\}, ..., \{F_e^{t-1}, F_p^{t-1}\}\}. \tag{5}$$

The pose of the LiDAR sensor in each feature set is used as the node of the pose map, and $\{F_e^t, F_p^t\}$ is used as the measurement value. Selecting k feature sets from M^{t-1} to construct $\bar{Q}^{t-1}$

$$\bar{Q}^{t-1} = \{\{F_e^{t-k}, F_p^{t-k}\}, \{F_e^{t-k-1}, F_p^{t-k-1}\}, \cdots, \{F_e^{t-1}, F_p^{t-1}\}\}. \tag{6}$$

Then, the pose constraints between $\{F_e^t, F_p^t\}$ and $\bar{Q}^{t-1}$ are obtained by the LM optimization method and added to the pose map.

Finally, the Iris-based loop closure detection method is used to eliminate the drift during the map construction process, and the constraint T_{cur}^{loop} between the current frame and the loop closure frame is added to the pose map. The back-end optimization process is implemented by Georgia Tech Smoothing and Mapping (GTSAM) [5].

3. Vehicle Localization Based on Point Cloud Map Matching

After the construction of point cloud map, when the vehicle drives into the map area again, the accurate position can be obtained by matching the current point cloud information with the existing map. However, the traditional point cloud map matching method has the problem of slow matching speed. In this paper, the RANSAC method [4] is adopted to remove the ground point cloud in the current frame. The point clod map constructed by Iris-LOAM has the problems of large data volume and low loading efficiency. In this paper, the constructed map is gridded and down-sampled, then the NDT matching method is used to match the processed current point cloud with the constructed point cloud map to obtain the current position of the vehicle. The framework of vehicle position estimation based on point cloud map matching is shown in Figure 2.

Figure 2
The framework for vehicle location estimation based on point cloud map

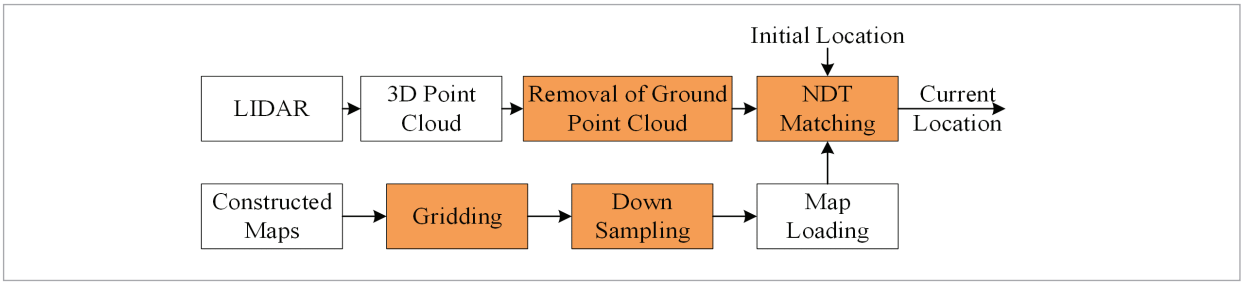

The initial manuscript and all the edited versions, if there will be any, should be uploaded by using the same paper ID and a specific user name and password. Papers that are simply sent to our e-mail but not uploaded on the website, will not be considered.

3.1. RANSAC-based ground Point Cloud Removal Method

The point cloud acquired by LiDAR contains a large amount of ground information, which has strong similarities and has limit effect on positioning. Traditional point cloud map matching methods do not remove the ground point cloud, and the matching efficiency is low. The effect of ground point cloud on matching efficiency is more severe in complex motion states. To improve the efficiency of point cloud map matching, the RANSAC method is adopted to remove the ground point cloud.

RANSAC uses an iterative approach to estimate the ground model parameters from the point cloud frames containing ground point cloud and non-ground point cloud data. The RANSAC method is easy to implement and operates efficiently for removing ground point clouds. The specific implementation steps are as follows:

1 Select three points from the current point cloud frame to estimate the ground model.

2 Calculate the ground model based on the three selected points:

$$a_p X_p + b_p Y_p + c_p Z_p + d_p = 0, \tag{7}$$

where a_p, b_p, c_p, and d_p are the coefficients of the plane equation, and (X_p, Y_p, Z_p) denotes the 3D coordinates of the laser point.

3 Calculate the distance D_{pi} from all points in the current point cloud frame to the ground model

$$D_{pi} = \frac{|a_p x_i + b_p y_i + c_p z_i + d_p|}{\sqrt{a_p^2 + b_p^2 + c_p^2}}, \tag{8}$$

where (x_i, y_i, z_i) is the 3D coordinate of the laser point. For the distance threshold D_{p_th}, if $D_{pi} < D_{p\_th}$, the point is considered to be inside the ground and the number of ground points that are inside the ground model is counted.

4 Compare the number of ground points in the current ground model with the number of ground points in the historical ground model, and record the model parameters with the largest number of ground points and the number of ground points;

5 Repeat steps (1)~(4) until the end of the iteration;

6 Remove all ground points from the current point cloud frame.

3.2. 3D NDT-based Point Cloud Map Matching Method

The NDT method is efficient and robust in point cloud matching. The 3D NDT method is insensitive to subtle transformations in the environment. Thus, the NDT method is used to obtain the location of the vehicle.

The completed point cloud map constructed by Iris-LOAM occupies a large storage space. If the completed point cloud map is loaded directly, it will consume a lot of time and reduce the matching efficiency. Thus, the completed map is gridded to reduce the loading time. In this paper, the whole map is divided into m sub-maps with $a_{sub} \times a_{sub}$ meter size.

To further improve the efficiency of point cloud map matching, the point cloud map is down sampled using the Voxel Grid (VG) [13] method, which can retain sufficient point cloud shape features while reducing the amount of point cloud data. The voxel is an extension of a two-dimensional pixel in three-dimensional space and is a set of cubic cells distributed in an orthogonal grid. The input point cloud map is divided into a 3D voxel grid with side length a_{vg}. The voxel A_{vg} contains S_{vg} data points, and its center of mass $\overline{x}_{vg}$ is used as the representative, $\overline{x}_{vg}$ can be calculated as:

$$\overline{x}_{vg} = \frac{1}{s_{vg}} \sum_{i=1}^{s_{vg}} \boldsymbol{x}_i, \tag{9}$$

In order to obtain the location of the vehicle, the starting position and attitude of the vehicle should be calibrated.

It is worth to mention here that the pitch and roll angles of the vehicle generally change little, while the heading angle changes a lot. Thus, the initial value of the heading angle plays a decisive role in the accuracy of the NDT matching results. After obtaining the initial longitude, latitude, and altitude parameters of the vehicle, the initial position of the vehicle in the local horizontal coordinate system can be obtained through coordinate transformation.

The 3D NDT method is used to match the point cloud at moment k with the global point cloud map and the translation matrix t_{k-1}^{k} and rotation matrix R_{k-1}^{k} of the vehicle relative to the moment $k-1$ can be obtained. Then the position of the vehicle at moment k can be obtained through the position transformation:

$$\boldsymbol{P}_{map}^{n}(k) = \boldsymbol{R}_{k-1}^{k} \boldsymbol{P}_{map}^{n}(k-1) + \boldsymbol{t}_{k-1}^{k}, \tag{10}$$

where $\boldsymbol{P}_{\text{map}}^{n}(k) = [\, p_{map}^{E} \quad p_{\text{map}}^{N} \quad p_{\text{map}}^{D} \,]^{T}$.

4. Experimental Validation

To evaluate the localization performance of the proposed methodology, extensive experiments were conducted in Nanjing and Wuxi, China. Representative trajectories were chosen to show in this paper.

The 32-line LiDAR from Velodyne were mounted on the top of the vehicle. The data acquisition and processing platform is ARK-3520 industrial control computer produced by Advantech. Moreover, an accurate and reliable NovAtel SPAN-CPT system was used as a reference for quantitative comparison. The horizontal position accuracy of SPAN-CPT system was 0.01 m without GPS outages.

4.1. Performance Evaluation of the Point Cloud Map Construction Based on Iris-LOAM

After eliminating the noise points and outliers and removing the distortion in the point clouds, SC-LeGO-LOAM and Iris-LOAM are conducted to construct the point cloud map for comparative analysis. Analysis of the point cloud map construction based on Iris-LOAM

Figure 3(a)-(b) are two frames of point clouds scanned by LiDAR when passing the same position with different attitudes. Figure 3(c)-(d) are the LiDAR-Iris descriptors of the two frames. It can be seen from Figure 3 that there are rotation and translation transformations between the two frames of point clouds, and the corresponding iris descriptors are also globally unique. The LoG-Gabor filter and thresholding operation are adopted to further extract features from the iris descriptors, and the resulting binary feature map is shown in Figure 4. It can be seen from Figure 4 that the feature texture in the binary map extracted by the LoG-Gabor filter is similar to the human iris. The Fourier transform method is adopted to calculate the transformation relation between the two LiDAR-Iris descriptors in Figure 4 and the relation is applied to the iris descriptors. The obtained iris descriptors before and after the Fourier transformation are shown in Figure 5 Among them, the pictures in first and second rows are the iris descriptors of point cloud 1 and point cloud 2 before Fourier transformation, and the picture in the third row is the iris descriptor of point cloud 2 after Fourier transformation.

By comparing the pictures in the first row and the third row, the iris descriptor consistency of two frames is improved after Fourier transformation. Thus, it can be concluded that the iris descriptor can detect the loop-closure frames accurately.

Figure 3
The point cloud frame and its iris descriptor when the vehicle enters the loop-closure position with different attitudes

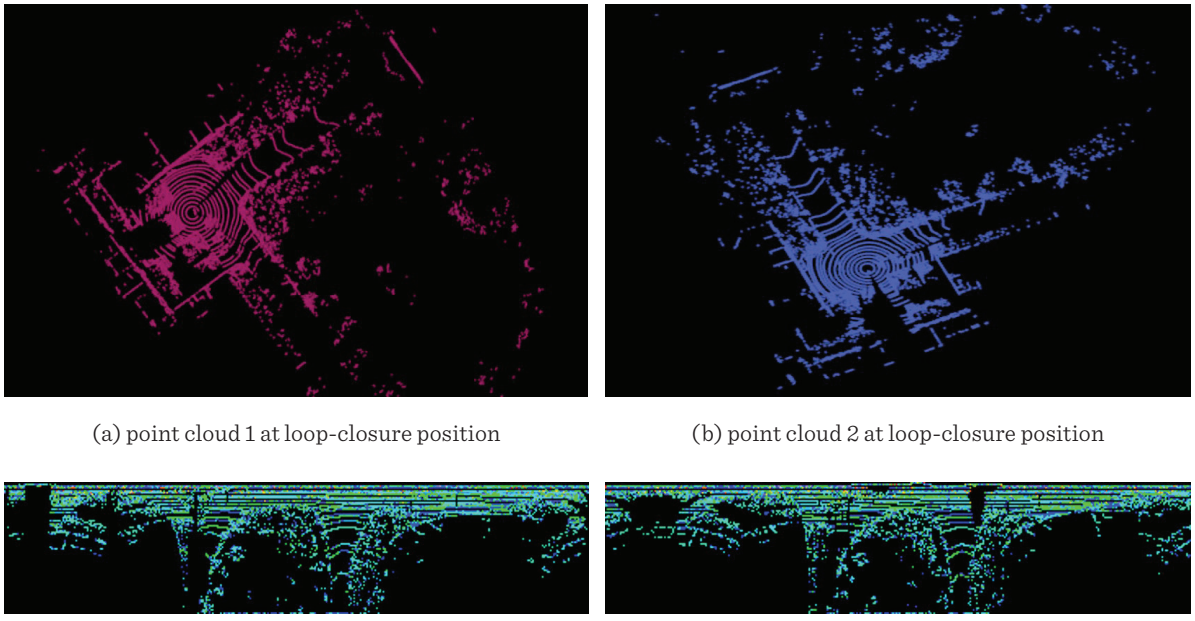

(a) point cloud 1 at loop-closure position

(b) point cloud 2 at loop-closure position

(c) LiDAR-Iris descriptor for point cloud 1

(d) LiDAR-Iris descriptor for point cloud 2

Figure 4
Binary feature maps of iris descriptors of point cloud

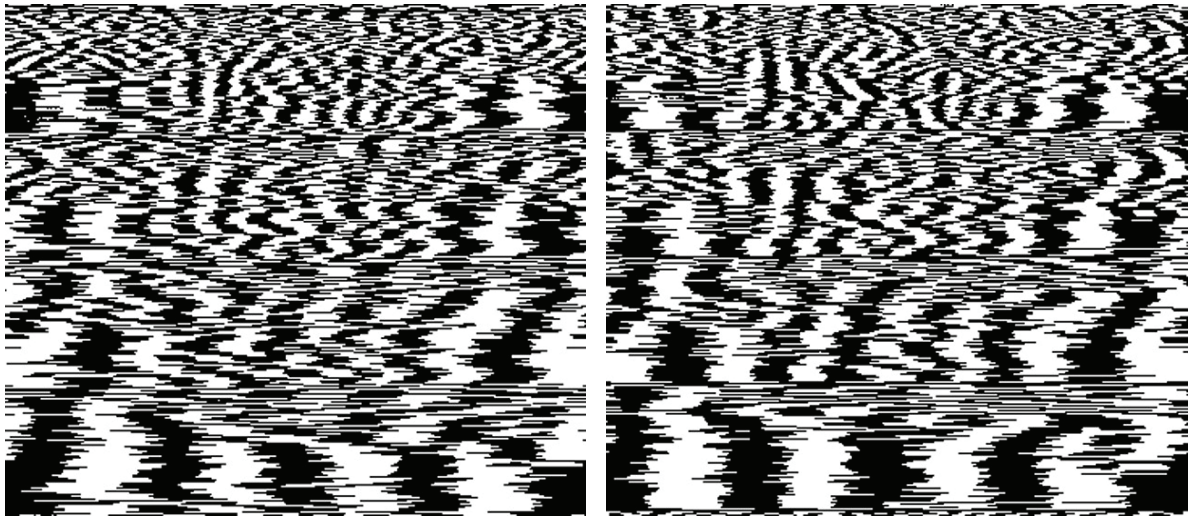

(a) Binary feature map of point cloud 1

(b) Binary feature map of point cloud 2

Figure 5
The point cloud frame and its iris descriptor when the vehicle enters the loop-closure position with different attitudes

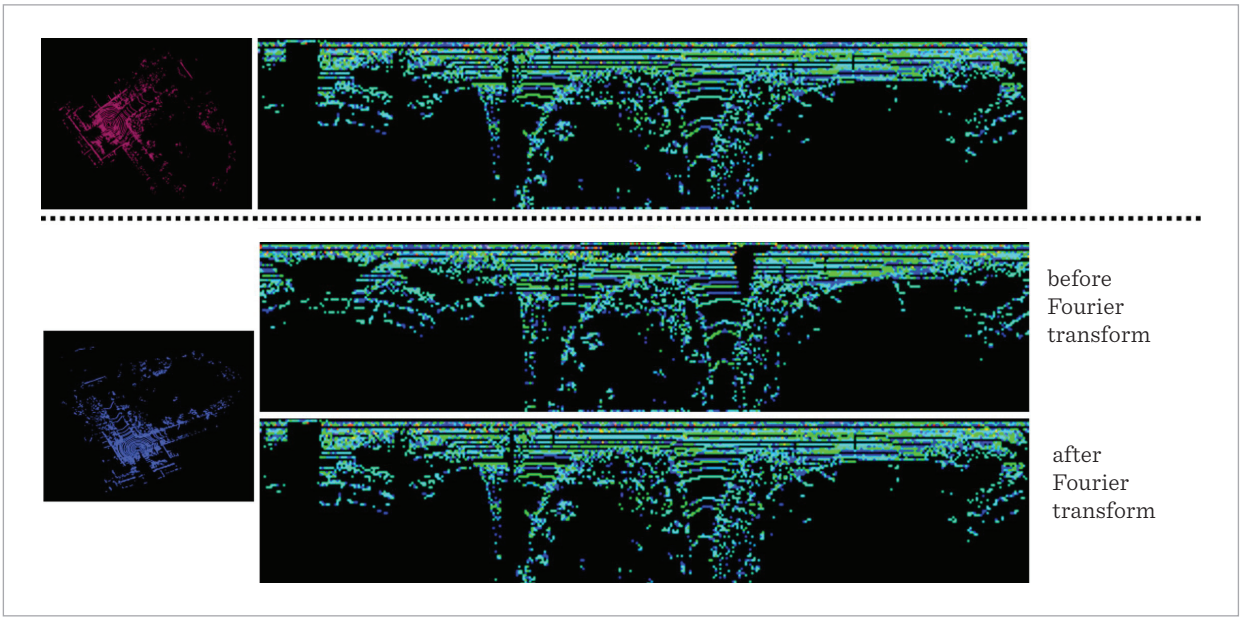

To validate the efficiency improvement of iris descriptor, this paper uses the iris descriptor and the SC descriptor to perform 100 loop-closure detections respectively and the time-consuming comparison is shown in Figure 6. The maximum time-consuming is 1853.57ms and minimum time-consuming is 237.34ms for Lidar-Iris descriptor. While the maximum time-consuming is 2405.87ms and minimum time-consuming is 730.12ms for Scan Context descriptor. The average time taken for 100 loop-closure detections using Scan Context descriptor and iris descriptor is 1505.6ms and 574.03ms, respectively. The average time using the iris descriptor is reduced by 61.9%. It can be concluded that using the iris descriptor for loop-closure detections takes less time and performs more efficiently

Figure 7 shows the point cloud maps constructed by SC-LeGO-LOAM and Iris-LOAM, respectively. It can be seen that the map constructed by the Iris-LOAM contains more detailed environmental information and are more precise than SC-LeGO-LOAM

Figure 6
Time-consuming comparison of loop closure detection by Iris and SC

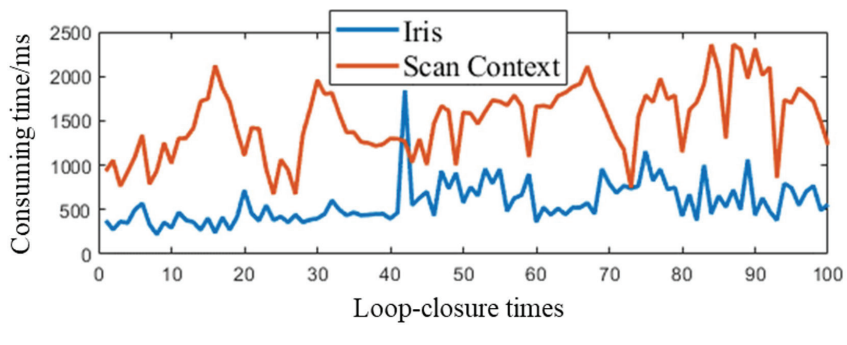

Figure 7
The point cloud maps of the test park constructed by Iris-LOAM and SC-LeGO-LOAM

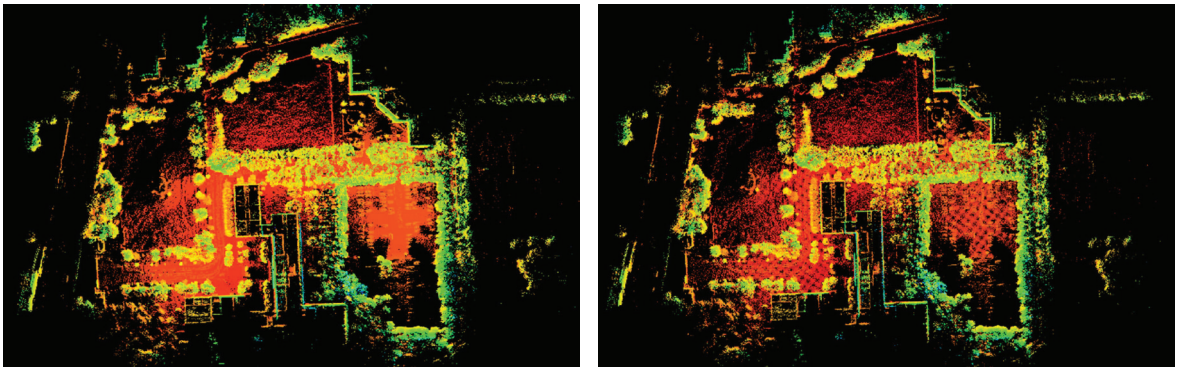

(a) Map constructed by Iris-LOAM (b) Map constructed by SC-LeGO-LOAM

4.2. Performance Evaluation of the Vehicle Localization Based on Point Cloud Map Matching

The test platform and scene of vehicle localization experiments based on point cloud map matching are consistent with the point cloud map construction experiments based on Iris-LOAM.

Figure 8 shows the effect of removing the ground point cloud based on the RANSAC method. It can be seen that the RANSAC method can effectively remove the ground point cloud. The consuming-time of map matching in the case of removing the ground point cloud and not removing the ground point cloud was counted, and the results are shown in Figure 9. The average time taken for map matching before and after removing the ground point cloud is 209.23ms and 126.50ms, respectively. The average map matching time after removing the ground point cloud is reduced by 39.5%. It can be concluded that the matching efficiency is improved after removing the ground point cloud.

Figure 8
Comparison of maps before and after removing the ground point cloud

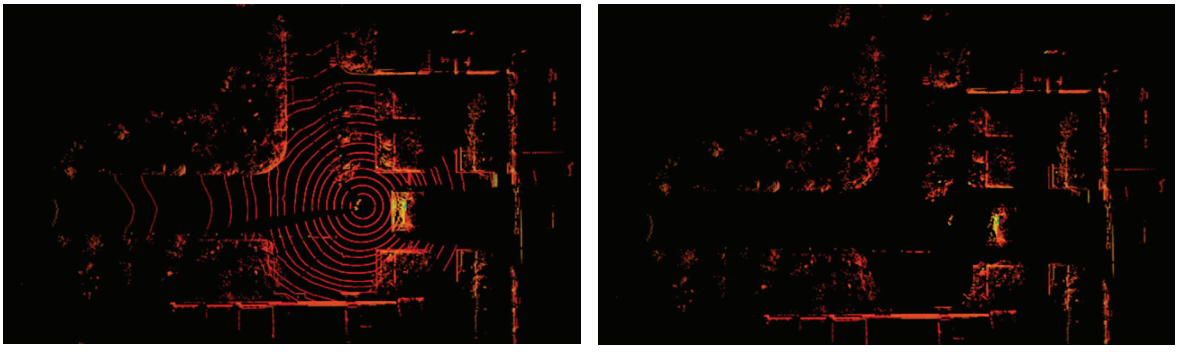

(a) Before removing the ground point cloud (b) After removing the ground point cloud

Figure 9
Time-consuming comparison of point cloud map matching

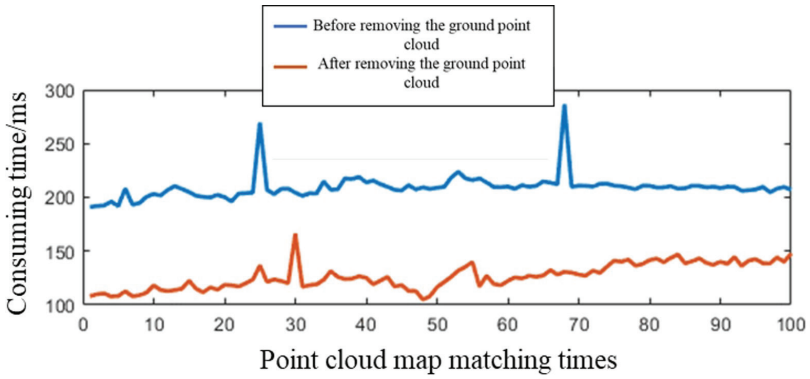

Figure 10
The results before and after processing the point cloud maps of test park

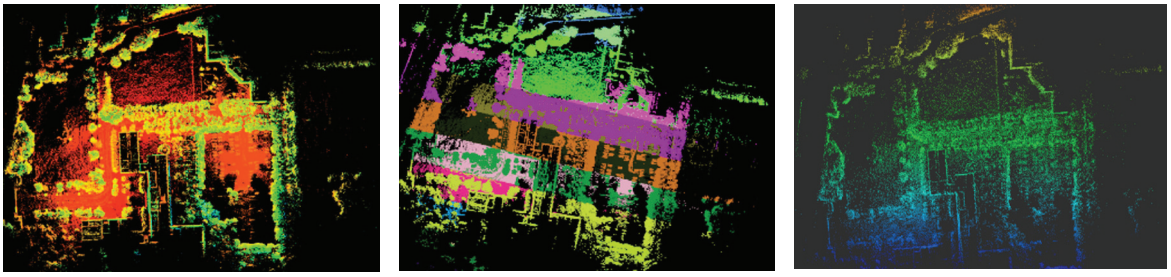

(a) map of raw point cloud (b) map after gridding (c) map after down-sampling

Figure 10 shows the results before and after processing the point cloud map. The griding operation is used to spatially divide the point cloud map. In order to display the result of gridded map, different colors are used to represent different submaps in Figure 10(b), and its side length is set to 50 meters during the experiments. The time taken for loading the point cloud map before and after gridding is 41704.1ms and 1851.81ms, respectively. The loading efficiency after gridding is improved by more than 22 times. It can be seen that using the grid method to process large-scale maps will greatly improve the point cloud map matching efficiency. In order to further improve the point cloud map matching efficiency, the Voxel Grid (VG) method is used to down sample the loaded gridded map, which can reduce the number of point clouds while retaining the map features. The down sampled map is shown in Figure 10(c).

After determining the initial position and attitude of the vehicle, NDT method is used to calculate the vehicle position. Figure 11 shows the point cloud map matching results of vehicle in the process of going straight and turning. The gray point cloud in the figure constitutes the historical point cloud map, while the colored point cloud constitutes the current point cloud frame. It can be seen from Figure 11 that the proposed localization method can achieve well point cloud map matching both during the straight-forward where the point cloud features change relatively gently and during the turning

Figure 11
Point cloud map matching results of vehicle in the process of driving

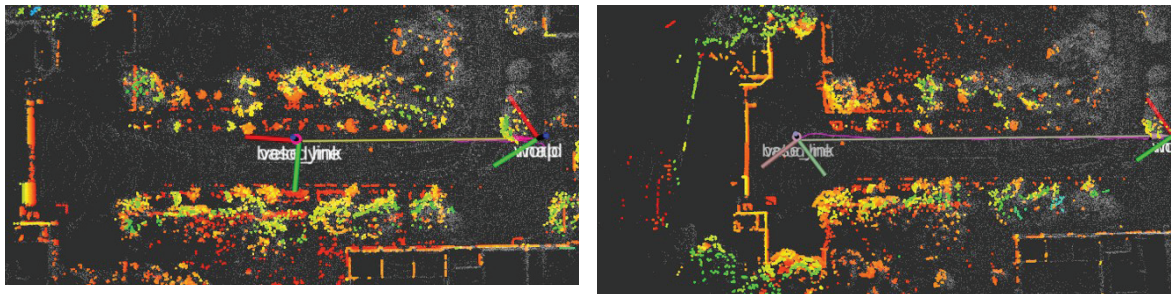

(a) Point cloud map matching during the straight driving (b) Point cloud map matching during turning

Figure 12
Localization results of the proposed methodology in trajectory 1

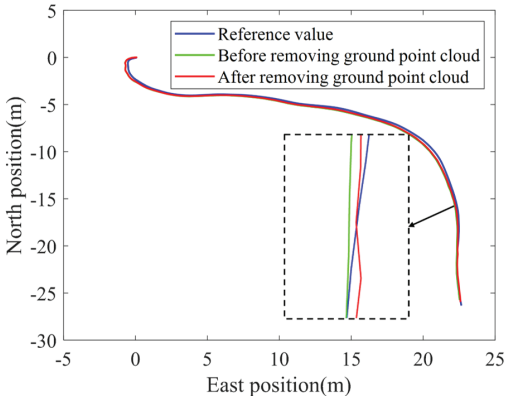

(a) Vehicle localization results

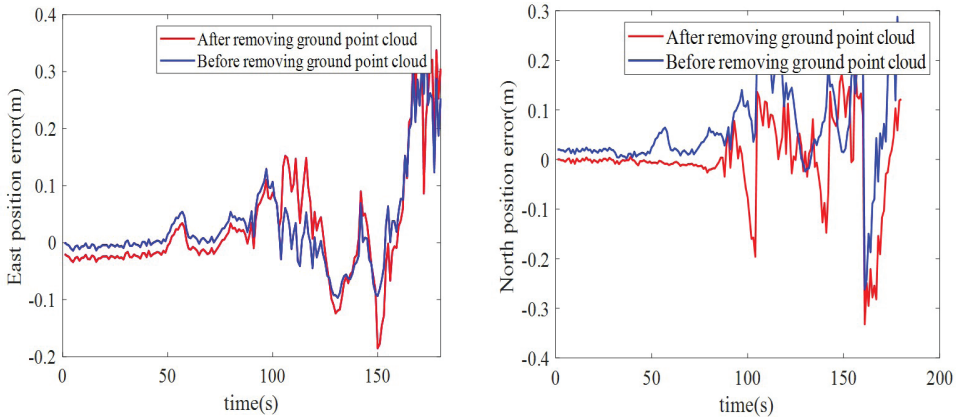

(b) Position errors before and after removing ground point cloud

where the point cloud features change drastically. The robustness and practicability of the proposed method is validated.

Finally, two representative trajectories are chosen to show the localization performance. Trajectory 1 is in the campus of Nanjing, while Trajectory 2 is in the National Intelligent Transportation Comprehensive Test Base in Wuxi. The localization results and Position errors are shown in Figure 12 and Figure 13, respectively. The statistics of position errors are illustrated in Table 1, including maximum, Mean Absolute (MA), and Root Mean Square (RMS) errors. The reference is from the high-precision integrated navigation system after Real-Time Kinematic (RTK) difference. It can be seen from Figures 12-13, and Table 1 that the vehicle position accuracy before and after removing the ground point cloud is similar, which indicates that removing the ground point cloud will not affect the accuracy of the positioning results. Therefore, the improved point cloud map matching algorithm in this paper can efficiently estimate the localization information of the vehicle.

Figure 13

Localization results of the proposed methodology in trajectory 2

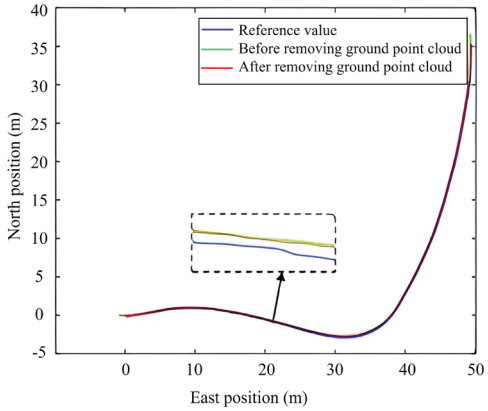

(a) Vehicle localization results

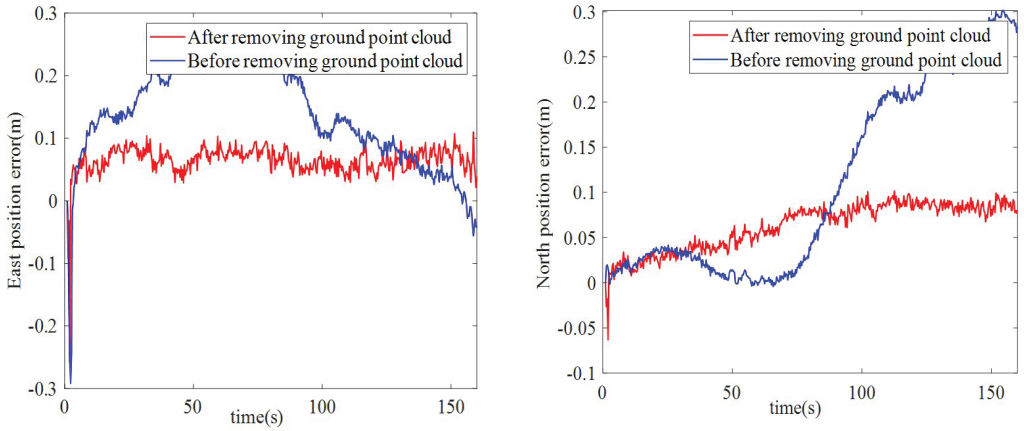

(b) Position errors before and after removing ground point cloud

Table 1
Statistics of position errors for the two trajectories

Errors(m)		Before removing the ground point cloud			After removing the ground point cloud		
		Max	MA	RMS	Max	MA	RMS
Trajectory 1	East position	0.313	0.129	0.135	0.332	0.134	0.141
	North position	0.282	0.152	0.159	0.340	0.149	0.157
Trajectory 2	East position	0.292	0.118	0.122	0.245	0.093	0.095
	North position	0.299	0.111	0.113	0.095	0.074	0.085

4.3. Discussion

1 The advantage of Lidar-Iris descriptor. The bird's eye view of each point cloud frame scanned by the LiDAR is centered on the body of the vehicle and the surrounding point cloud is distributed in a circular pattern, which is similar to the iris of the human eye. In this paper, the texture features are extracted from Lidar-Iris descriptor through the LoG-Gabor filter. The extracted binary feature map is beneficial to improve the accuracy of loop-closure detection and mapping. However, the SC descriptor only encodes the maximum height information of the environment and neglects the feature extraction step for the height. Thus, the map constructed by Iris-LOAM has higher accuracy than that constructed by the SC-LeGO-LOAM.

   In addition, the Lidar-Iris descriptor performs loop-closure detection by using the extracted binary feature, while the SC descriptor adopts a brute force matching method. The Iris-LOAM is less time-consuming and more efficient in loop-closure detection than using SC descriptor.

2 Whether to remove the ground point cloud when constructing the map. Removing the ground point cloud during the map matching procedure can improve the efficiency without compromising accuracy. However, from the point of view of integrity, the ground point cloud should be retained when building the map, as they are also part of the map. If the point cloud map is dedicated to positioning, the ground point cloud can be removed during the construction procedure.

5. Conclusion

This paper improves the efficiency of vehicle localization based on LiDAR place recognition from two aspects, i.e. map construction and map matching. First, the Iris-LOAM map construction method is proposed to improve the loop-closure detection module of LOAM by using the LiDAR-Iris global descriptor and NDT registration algorithm. Further, to improve the efficiency of the traditional NDT-based point cloud map matching method, the RANSAC algorithm is adopted to remove the ground point cloud in the current frame, and the grid and voxelization operations are used for the large-scale point cloud map. The matching speed can be greatly improved while ensuring the matching accuracy.

The experimental results show that the Iris-LOAM algorithm can efficiently and accurately construct the large-scale point cloud maps, and the improved NDT matching algorithm can efficiently estimate the vehicle position. Future work will focus on fusing LiDAR with other sensors to improve the applicability of LiDAR place recognition to large scale traffic environments.

Acknowledgement

This work is supported by the Opening Project of Key Laboratory of Technology on Intelligent Transportation Systems, Ministry of Transport, Beijing, China (Grant No. F20211748), the National Natural Science Foundation of China (Grant No. 41904024), and ZhiShan Scholar Program of Southeast University.

References

1. Agachai, S., Hung, W. H. Smarter and More Connected: Future Intelligent Transportation System. IATSS Research, 2018, 42(2), 67-71. https://doi.org/10.1016/j.iatssr.2018.05.005
2. Agarwal, R., Jalal, A. S., Arya, K. V. Local Binary Hexagonal Extrema Pattern (LBHXEP): A New Feature Descriptor for Fake Iris Detection. The Visual Computer, 2021, 37, 1357-1368. https://doi.org/10.1007/s00371-020-01870-0
3. Falco, G., Pini, M., Marucco, G. Loose and Tight GNSS/INS Integrations: Comparison of Performance Assessed in Real Urban Scenarios. Sensors, 2017, 17(2), 255. https://doi.org/10.3390/s17020255
4. Han, X. F., Jin, J. S., Wang, M. J. A Review of Algorithms for Filtering the 3D Point Cloud. Signal Processing: Image Communication, 2017, 57, 103-112. https://doi.org/10.1016/j.image.2017.05.009
5. Jimenez, R., Ivan, D. D. A Factor Graph Approach to Constrained Optimization, 2017.
6. Jin, S., Wang, Q., Dardanelli, G. A Review on Multi-GNSS for Earth Observation and Emerging Applications. Remote Sensing, 2022, 14(16), 3930. https://doi.org/10.3390/rs14163930
7. Li, X., Xu, Q. M., Wang, M. A. Simultaneous Viewpoint- and Condition-Invariant Loop Closure Detection Based on LiDAR Descriptor for Outdoor Large-Scale Environments. IEEE Transactions on Industrial Electronics, February, 2022, 70(2), 2117-2127. https://doi.org/10.1109/TIE.2022.3163511
8. Li, X., Xu, Q. M. A Reliable Fusion Positioning Strategy for Land Vehicles in GPS-Denied Environments Based on Low-Cost Sensors. IEEE Transactions on Industrial Electronics, 2017, 64(4), 3205-3215. https://doi.org/10.1109/TIE.2016.2637306
9. Nunes, C. F. G., Pádua, F. L. C. A Local Feature Descriptor Based on Log-Gabor Filters for Keypoint Matching in Multispectral Images. IEEE Geoscience and Remote Sensing Letters, 2017, 14(10), 1850-1854. https://doi.org/10.1109/LGRS.2017.2738632
10. Shi, X. Y., Peng, J. J., Li, J. P. The Iterative Closest Point Registration Algorithm Based on the Normal Distribution Transformation. Procedia Computer Science, 2019, 147, 181-190. https://doi.org/10.1016/j.procs.2019.01.219
11. Sun, X. L., Guan, H. C., Su, Y. J. A Tightly Coupled SLAM Method for Precise Urban Mapping. Acta Geodaetica et Cartographica Sinica, 2021, 50(11), 1585-1593. https://doi.org/10.11947/j.AGCS.2021.20210243.
12. Vincent, H., Damien, H., Philibert, N., Zhu, X. A Novel Hybrid Approach Based-SRG Model for Vehicle Position Prediction in Multi-GPS Outage Conditions. Information Fusion, 2018, 41, 1-8. https://doi.org/10.1016/j.inffus.2017.07.002
13. Xiong, B., Jiang, W., Li, D., Qi, M. Voxel Grid-Based Fast Registration of Terrestrial Point Cloud. Remote Sensing, 2021, 13(10), 1905. https://doi.org/10.3390/rs13101905
14. Xu, X., Zhang, L., Yang, J. A Review of Multi-Sensor Fusion SLAM Systems Based on 3D LIDAR. Remote Sensing, 2022, 14(12), 2835. https://doi.org/10.3390/rs14122835
15. Yurtsever, E., Lambert, J., Carballo, A., Takeda, K. A Survey of Autonomous Driving: Common Practices and Emerging Technologies. IEEE Access, 2020, 8, 58443-58469. https://doi.org/10.1109/ACCESS.2020.2983149
16. Zhou, Y., Wang, Y., Poiesi, F. Loop Closure Detection Using Local 3D Deep Descriptors. IEEE Robotics and Automation Letters, 2022, 7(3), 6335-6342. https://doi.org/10.1109/LRA.2022.3156940
17. Zhu, Y. J., Chen, Q. J., Zhang, H. A SLAM Method Based on LOAM for Ground Vehicles in the Flat Ground. 2019 IEEE International Conference on Industrial Cyber Physical Systems (ICPS), 2019, 546-551. https://doi.org/10.1109/ICPHYS.2019.8780378